Materials Science-Poland, *Vol. 26*, *No. 3*, *2008*

Dry sliding wear characteristics of 0.13 wt. % carbon steel

V.K. GUPTA[1*], S. RAY[2], O.P. PANDEY[3]

[1]Mechanical Engineering, University College of Engineering,
Punjabi University, Patiala (Pb.) 147 002, India

[2]Department of Metallurgical and Materials Engineering,
Indian Institute of Technology, Roorkee (U.A.) 247 667, India

[3]School of Physics and Material Science, Thapar University,
Patiala (Pb.) 147 004, India

Wear characteristics of 0.13 wt. % plain carbon steel, heat treated under various conditions, were monitored on a standard pin-on-disk wear testing machine under the normal loads of 2.5, 4.5 and 5.5 kg and at a constant sliding velocity of 1 m/s. Weight loss of the specimen was measured at various time intervals to obtain wear rate. The variation in volume loss with sliding distance indicated the presence of run-in wear followed by steady state wear. The wear mechanism was found to be primarily oxidative in nature, which was confirmed by the analysis of worn surfaces and wear debris generated during sliding. Wear resistance was found to be dependent on the microstructure and morphology of the phases. The wear coefficients calculated for various heat-treated specimens revealed that the ferrite-coarse pearlite, ferrite-fine pearlite, ferrite-tempered martensite and ferrite martensite structures show the wear resistance in decreasing order.

Key words: steel; sliding wear; wear coefficient

1. Introduction

Plain carbon steels consisting of about four-fifths of the total tonnage of steel production, are economical compared to alloy steels. These are extensively used as structural components for many engineering applications. Among many failure modes associated with steel components, wear presents a unique challenge to the designer and the developer of mechanical components. Wear characteristics of steel components and their real life performance under various working environments have been the

[*]Corresponding author, e-mail: guptavk_70@yahoo.co.in

subject of numerous investigations [1–19]. Because so many variables are involved, such as load, sliding speed, test geometry, composition, hardness, environment etc., controversies over the understanding of wear mechanism still exist, as these parameters are interdependent variables. In addition to these variables, the type of microstructure also influences the wear resistance of steel. Although several investigations have demonstrated an improvement in wear resistance of steel through surface hardening treatments and surface alloying [20], very few studies have been done to correlate the wear properties of steel with its microstructure [2, 5–8, 10–17]. Wayne and Rice [2] have revealed the dependence of wear on microstructure and have concluded that the dual phase (DP) steel, consisting of hard martensite islands embedded in a relatively soft and ductile ferrite matrix, offers higher wear resistance than that observed in steel with spheroidal carbides. The wear resistance of DP steel was found to depend on the volume fraction of martensite. Similar observations have also been reported by Tyagi et al. [12]. Sawa and Rigney [5] have shown that the wear behaviour of DP steel also depends strongly on morphology (i.e., shape, size and distribution) of its martensite phase. Tyagi et al. [11] have found that ferrite–martensite structure exhibits higher wear resistance compared to ferrite–fine pearlite structure. In our earlier study [10] on wear behaviour of near eutectoid steel containing 0.86 wt. % carbon, it was observed that coarse pearlite structure possesses better wear resistance compared to fine pearlite and tempered martensite structure.

In the present investigation, an attempt is made to study the influence of microstructure in hypoeutectoid steel containing 0.13 wt. % of carbon on its wear characteristics under dry sliding condition at different loads and at a fixed sliding speed at room temperature, using a standard pin-on-disk wear testing machine. The idea of selecting this composition was to observe the variation in wear characteristics with variation in carbon contents and to compare the results with those of our earlier study for nearly eutectoid steel [10].

2. Experimental

Commercial grade steel containing C (0.13 wt. %), Mn (0.62 wt. %), Si (0.08 wt. %), P (0.048 wt. %) and S (0.035 wt. %) was used in the present investigation. The steel samples were subject to various heat treatment processes to attain variety of microstructures. The wear characteristics of heat-treated samples were investigated. The details of experimental procedures are described below.

Heat treatment of samples. In order to compare the results of our earlier study [10] samples of similar size, 30 mm long and 6.25 mm in diameter were cut from a steel bar. Four sets comprising three pins in each set were taken for carrying out heat treatment. All sets of samples were heated in a tubular furnace to 840 °C in the ($\alpha + \gamma$) region for a period of 40 min. These samples were covered with cast iron chips to avoid oxidation. After heating, three sets of samples were taken out of the furnace.

The first set was allowed to cool in air to develop ferrite-fine pearlite structure and the remaining two sets were directly quenched in water to develop dual phase microstructure containing martensite in a matrix of ferrite. Out of these two sets of water quenched samples, one set was further subject to high temperature tempering treatment at 640 °C for two hours followed by water quenching resulting in ferrite-tempered martensite structure. The fourth set was allowed to cool inside the furnace up to room temperature to attain ferrite-coarse pearlite structure. In the present study, the deviation from conventional normalising and annealing treatment by cooling from the intercritical annealing temperature range (i.e., $\alpha + \gamma$ region) was done to keep similar ferrite areas in the steel subject to various heat treatments. The bulk hardness of the heat-treated samples was measured at a load of 20 kg on calibrated Vickers hardness-testing machine using a diamond pyramid indenter, and is reported in Table 1.

Table 1. Hardness of 0.13 wt. % carbon steel heat treated under various conditions

Sample	VHN
Annealed	99
Normalized	108
Intercritically annealed and quenched	161
Intercritically annealed, quenched and tempered	134

Metallographic studies. The heat-treated samples were prepared for metallographic studies by grinding them on belt grinder driven by an electric motor. These samples were further polished up to 4/0 grade (~38 μm) of emery paper followed by cloth polishing using submicron size alumina paste. After polishing, the samples were etched with 2% nital and analysed under optical and scanning electron microscope. Volume fractions of phases present in samples were estimated by the point counting method [21]. Microhardness of phases present in the heat-treated samples was measured using 0.005 kg load on the Vickers scale, and is reported in Table 2.

Table 2. Microhardness (measured at 0.005 kg load) and volume fraction of phases in heat-treated samples

Sample	Phase present	Microhardness [VHN]	Volume fraction of the phase
Annealed	ferrite	174	0.84
	pearlite (coarse)	280	0.16
Normalized	ferrite	184	0.79
	pearlite (fine)	420	0.21
Intercritically annealed and quenched	ferrite	280	0.69
	martensite	552	0.31
Intercritically annealed, quenched and tempered	ferrite	195	0.80
	tempered martensite	276	0.20

Wear test. Wear tests were conducted using polished pin samples with flat surfaces in the contact region but rounded in the corner and cleaned with acetone to remove dust or grease from the surfaces. Dry sliding wear tests were carried out against the counterface of a hardened and polished disk made of EN-32 steel having HRC from 62 to 65 at a relative humidity of 50–70% at room temperature of 35 °C.

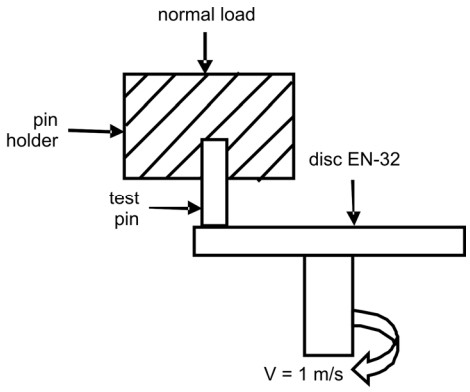

Fig. 1. Test geometry of Pin-on-disc wear testing machine

A sturdy pin-on-disk machine supplied by DUCOM, Bangalore (India), as shown schematically in Fig. 1, was used to carry out the wear tests. Pin weight losses were measured at various time intervals, using an electronic balance having an accuracy of 10^{-7} kg. Weight losses were converted to volume losses by dividing the weight by the density of steel. Initially, the weight loss of the pin was measured after every 2 min of sliding, for up to 16 min, and thereafter, at the intervals of 15 min for a total sliding period of 3 h. The tests were conducted at the loads of 2.5, 4.5 and 5.5 kg, and at a constant sliding velocity of 1 m/s. Each test at a given load and sliding velocity was repeated three times, with identical new samples on a fresh disk surface, and the average data for volume loss after each time interval were used for the analysis of wear rate. The wear debris obtained after the initial 16 min of sliding as well as after each test run were examined under SEM. The worn surfaces of the samples were also examined under SEM to know the wear mode of the worn surfaces.

3. Results and discussion

3.1. Microstructural characteristics of pin specimens

The microstructures of the heat-treated samples were examined under optical and scanning electron microscope. Figures 2a1 and 2a2 show the microstructure of the

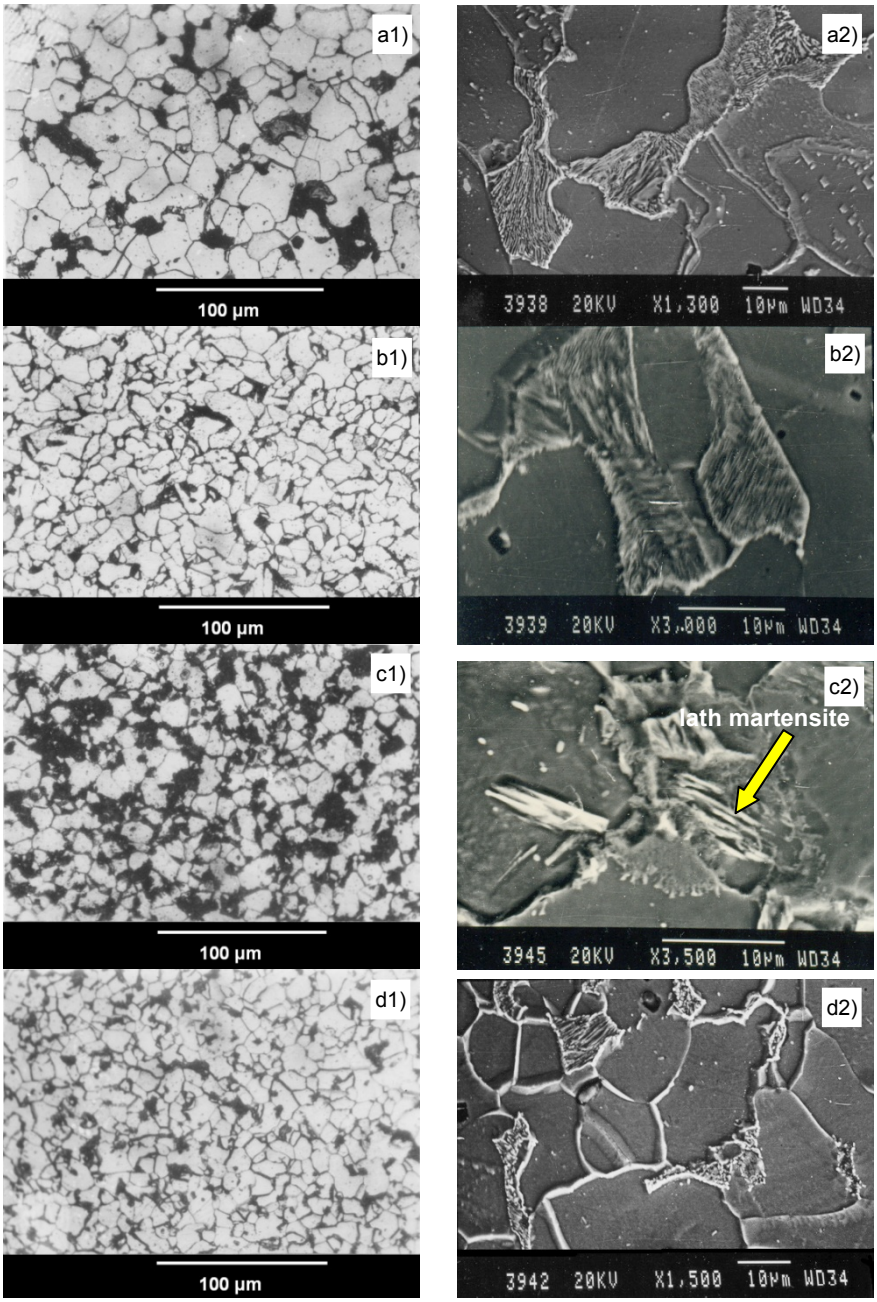

Fig. 2. Micrographs (1 – optical, 2 – SEM) of steel samples: a) annealed (AD), b) normalized (ND) c) intercritically annealed and quenched (IQ), d) intercritically annealed, quenched and tempered (IT)

annealed sample, revealing the presence of ferrite (bright areas) and of pearlite (dark areas). However, the structure of pearlite could be clearly seen in Fig. 2a2 at higher

magnification. The ferrite grain size is observed to vary from 10 to 20 μm. The volume fractions of ferrite and pearlite as observed from point counting method are 0.84 and 0.16, respectively. Figures 2b1 and 2b2 show the normalized ferrite-fine pearlite microstructures examined under optical microscope and SEM at various magnifications. The sample has bright areas of ferrite and dark areas of pearlite as observed at low magnification, but the pearlite could be resolved at a higher magnification in most of the areas. The volume fraction of pearlite is 0.21, as compared to 0.16 in the annealed sample. The ferrite grain size is observed in the 6–12 μm range, and is finer than that observed in the annealed sample. The ferrite–martensite microstructures of the sample intercritically annealed at 840 °C and quenched in water is shown in Figs. 2c1 and 2c2. Bright areas of ferrite and dark areas of martensite are evident in Fig. 2c1 but at higher magnification a coarser lath type of martensite could be observed inside the dark areas, Fig. 2c2. The microhardnesses of the dark and bright areas are found to be 552 VHN and 280 VHN, respectively (Table 2) which correspond to the hardness of martensite and ferrite in DP steel of similar composition [2]. The volume fractions of ferrite and martensite phases are 0.69 and 0.31, respectively. However, in some of the reports on steel containing higher carbon percentage, the hardness of martensite phase reported is on the higher side [11, 12]. This indicates that a complete transition of pearlite-austenite into martensite has not occurred, which is also evident in microstructures. Figures 2d1 and 2d2 show ferrite-tempered martensite microstructures of intercritically annealed and quenched samples followed by tempering at 640 °C for 2 h. It could be noticed that the volume fraction of dark etching martensite area has reduced to about 0.20 compared to that observed in the quenched sample, as is shown in Fig. 2c1. The microstructure observed under SEM, as shown in Fig. 2d2, clearly reveals tempered carbides in certain areas, but still there are some areas where one could observe lath martensite.

3.2. Wear characteristics

The dependences of cumulative wear volume on the sliding distance under various normal loads and at a fixed sliding velocity of 1 m/s are shown in Figs. 3a–d for annealed (AD), normalized (ND), intercritically annealed and quenched (IQ), and intercritically annealed, quenched and tempered (IT) steels, respectively.

The cumulative wear volume loss with the sliding distance under different normal loads of 2.5, 4.5 and 5.5 kg has demonstrated a sub-linear variation, with coefficients of correlation exceeding 0.975 at all normal loads for all the steel samples. However, the data can be analyzed on a linear scale using two separate stages of wear behaviour characterized by two different linear segments. The change in slope has been observed after first 4 to 7 experimental points (first stage run-in) with last point common between both the linear segments. Both the lines have been determined by the linear least squares fit. The slope of the line gives the wear rate. The procedure followed helps to establish the run-in period rate (first stage) separately from the long-term steady-state rate (second stage).

For AD steel, the first linear segment (run-in) is found to be steeper compared to the second linear segment (steady state). A similar variation has been observed for ND, IQ and IT steels, as shown in Figs. 3b–d, respectively. The two stage linear wear trend has also been reported by other investigators [2, 10–12, 22–26] in different steels.

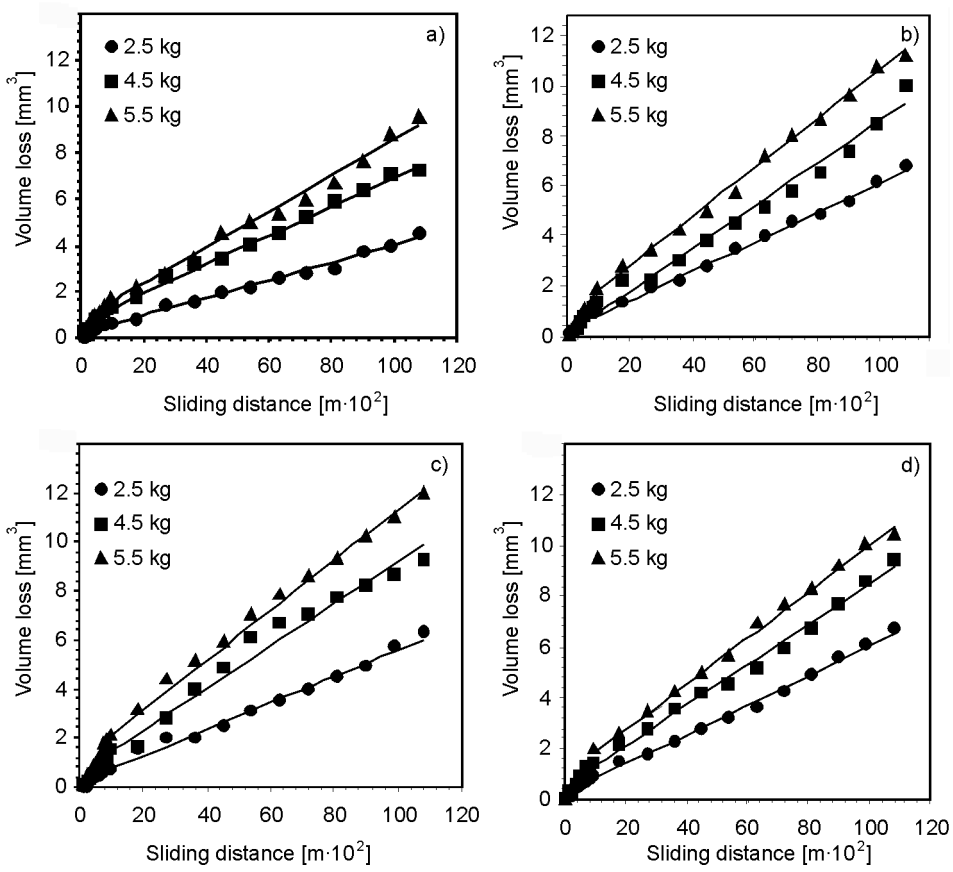

Fig. 3. Dependence of volume loss on the sliding distance for: a) AD, b) ND, c) IQ, d) IT steel specimen at various loads and a constant sliding velocity of 1 m/s

The wear rates of the samples at various loads have been determined from the slopes of the linear segments of Figs. 3a–d. Wear rates for both the linear segments are observed to increase almost linearly with load for all the heat-treated steel specimens, as shown in Figs. 4a, b. The observed linear variation of wear rate with load is indicative of Archard's wear law [10]. At a given load, the second linear segment shows a relatively lower wear rate compared to the first linear segment, for all the steel samples, as is evident from comparing Fig. 4a with 4b. Except for the load of 2.5 kg, the wear rate increases in the following order: AD, IT, ND and IQ for both the linear segments as shown in Figs. 4a, b. At a normal load of 2.5 kg, the wear rate corresponding

to first linear segment is relatively higher for ND steel compared to other steel specimens, which have almost equal values of wear rate, as shown in Fig. 4a. The wear rate corresponding to the second linear segment at a normal load of 2.5 kg is significantly lower in AD steel compared to those observed in other steel specimens (Fig. 4b). The steady state wear rate at a relatively lower load of 2.5 kg is almost similar in ND and IT steels but slightly higher than in IQ steel (Fig. 4b). Therefore, in terms of wear rates of both the segments ferrite–coarse pearlite structure is superior to ferrite–fine pearlite at all the loads. The ferrite-tempered martensite structure results in lower wear rates compared to the ferrite–martensite structure at higher loads of 4.5 and 5.5 kg. But, at a lower load of 2.5 kg, the ferrite-martensite structure has slightly lower wear rate in the second segment compared to the ferrite–tempered martensite structure, whereas in the first segments both the specimens have almost equal wear rates. At higher loads of 4.5 and 5.5 kg, the ferrite–tempered martensite appears to have an even better structure than ferrite–fine pearlite, in terms of wear rates of both the segments.

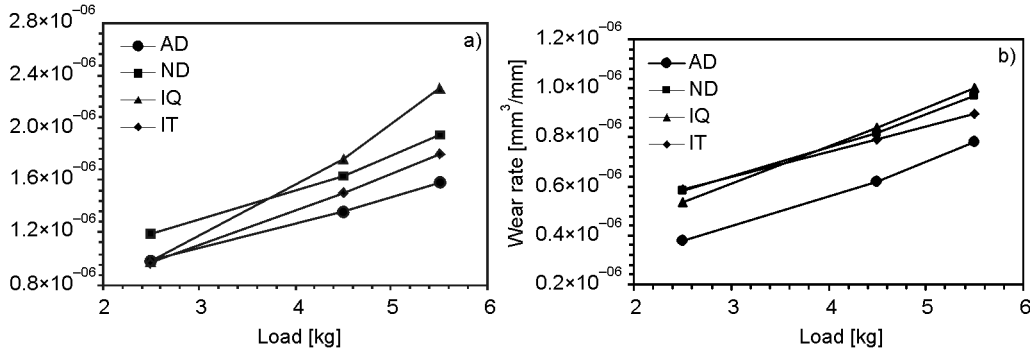

Fig. 4. Dependence of wear rate on load for heat-treated samples corresponding to: a) first linear segment, b) second linear segment

The wear coefficients have been obtained at different loads for AD, ND, IQ, and IT steels and are reported in Table 3. The wear coefficients are calculated using Archard's wear law

$$V = \frac{kWS}{3H}$$

where V is the volume loss in wear, W – the applied load, S – the sliding distance, H – the bulk hardness and k – the wear coefficient of the material [10]. The wear coefficients are estimated by dividing the wear rate (V/S) by the contact area (W/H), estimated from the applied load and indentation hardness, and multiplying the result by the geometrical factor of three. The first linear segment is observed to have a higher wear coefficient as compared to the second linear segment, for all the steel samples at different loads. Similar observations have also been made by some of the earlier investigators [10–12] on different steels.

Table 3. Wear coefficients corresponding to 1st (run-in) and 2nd (steady-state) segments

Sample	Linear segment	Wear coefficient ($k\times10^{-4}$) at loads of			Average ($k\times10^{-4}$)
		2.5 kg	4.5 kg	5.5 kg	
Annealed (AD)	1st	1.176	0.898	0.853	0.976
	2nd	0.451	0.409	0.421	0.427
Normalized (ND)	1st	1.545	1.174	1.149	1.289
	2nd	0.752	0.590	0.571	0.638
Intercritically annealed and quenched (IQ)	1st	1.891	1.890	2.020	1.934
	2nd	1.035	0.900	0.878	0.938
Intercritically annealed, quenched and tempered (IT)	1st	1.560	1.344	1.316	1.407
	2nd	0.942	0.705	0.654	0.767

3.3. Nature of wear surface and debris

Figures 5 and 6 show the SEM micrographs of the worn surfaces of the AD and IT steels, respectively, at different loads. The samples tested at low load of 2.5 kg are observed to be smooth, except for a few deep grooves as shown in Figs. 5(a) and 6(a), whereas at higher load of 5.5 kg worn surfaces are observed to have cracking, spalling, and thicker oxide cover, as shown in Figs. 5b and 6b. Therefore, it appears that

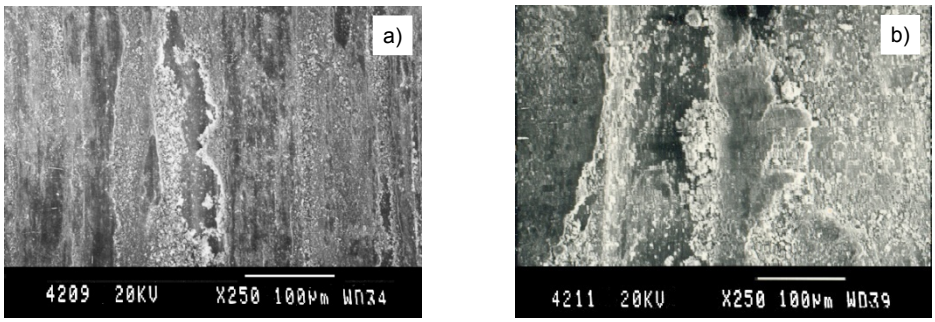

Fig. 5. SEM of worn surface of AD steel specimen tested at: a) 2.5 kg, b) 5.5 kg load

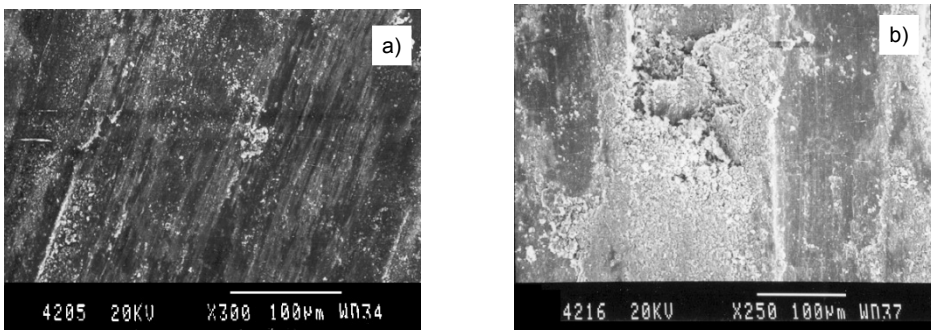

Fig. 6. SEM of worn surface of IT steel specimen tested at: a) 2.5 kg, b) 5.5 kg load

more oxide is generated at higher loads due to higher frictional heating, which leads to an increase in the temperature of the sliding surface. Glasscott et al. [23] in their study have also observed that oxide debris are generated during the process of wear which buildup progressively in the wear track as the contact pressure increases. During sliding, more and more oxide is produced, the metal–metal contact is reduced, thus lowering the wear rate, and leading to transition from severe to mild wear [9]. SEM micrographs of the worn surfaces also reveal the presence of scoring marks and areas of rough grooves in the direction of sliding. There are also a few craters seen in some areas where metallic particles have come into debris due to micro-welding or delamination, as shown in Fig. 5b. The adhesion effect is also visible at some places in Figs. 5b and 6b. In some samples, a flake-type morphological feature of the debris sticking to the surfaces is observed. These types of features have also been reported by other investigators [11, 27, 28]. The key features of all the tracks observed is that debris were observed to adhere at the worn surfaces in each specimen.

The wear debris collected for short sliding distances corresponding to the first linear segment have been compared under SEM with those obtained at long sliding distances corresponding to the second linear segment. A detailed analysis of all the debris collected for each sample corresponding to first and second linear segments have been performed. The common feature of the analysis performed for all the steel samples at each load corresponding to first linear segment indicates that oxidative wear is the dominating factor, as is evident from Fig. 7. The morphological features of the debris indicate that it is oxide in nature which is being formed in different stages, depending upon the availability of oxygen content. The reason for formation of oxide is that the surface gets exposed to atmosphere slowly as the load applied is relatively low.

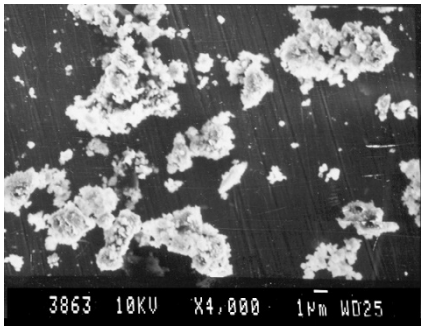

Fig. 7. SEM of wear debris corresponding to first linear segment for IQ steel specimen tested at 4.5 kg

As the load increases (corresponding to second linear segment), the volume fraction of the debris also increases. A detailed analysis of these wear debris have been done. Since the nature of debris corresponds to metallic and oxidative wear, thus only few micrographs have been presented for discussion (Figs. 8a–c). The samples tested at higher load in annealed conditions exhibit the features corresponding to metallic as well as oxidative wear (Fig. 8a). The flake type of morphology corresponds to metallic wear, whereas the round, rugged and coagulated features correspond to oxides. The

morphological features of the debris indicate that metal is removed from surface which gets oxidized during ploughing in the course of sliding. The ploughing marks are clearly visible on the surfaces of metallic debris (Fig. 8a).

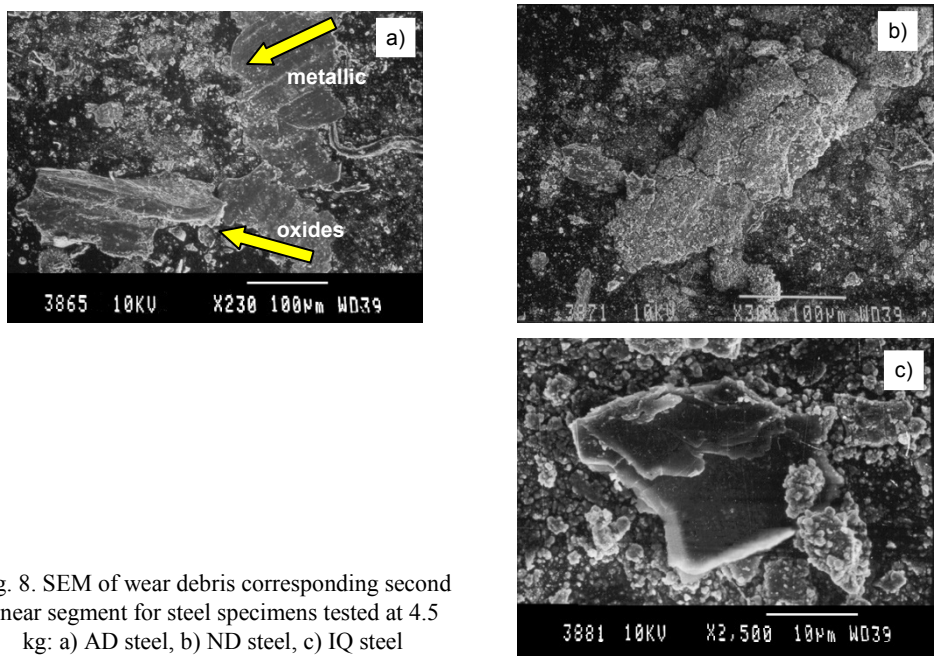

Fig. 8. SEM of wear debris corresponding second linear segment for steel specimens tested at 4.5 kg: a) AD steel, b) ND steel, c) IQ steel

Since annealed sample is very soft in nature, the metallic debris did not get oxidized so easily because of higher thermal conductivity of the phases present in it. The debris corresponding to normalized condition also indicates similar features (Fig. 8b). The loss of material due to the wear indicates that metallic debris get oxidized during sliding, as is evident from the micrograph shown in Fig. 8b. Fine cracks observed on the metallic surface of the debris further support our view that metal firstly comes out in the form of flakes, then it gets converted to oxides as the sliding distance increases. An important feature observed for debris obtained from IQ samples is that metallic wear dominates as compared to oxidative wear, as revealed from Fig. 8c. A typical morphological feature observed is that during the sliding, the debris get fragmented easily, leading to its transition to oxides at higher loads and higher sliding distances. The round spherical features of debris observed in Fig. 8c, which are partially oxidized, further supports this hypothesis. Since the loss of material in these steel samples is greater in comparison with other steel samples, it is obvious that some phases get easily detached from the matrix, as there is a vast difference between the coefficient of thermal expansion of ferrite and that of the martensite phase, which provides a conducive atmosphere for its easy detachment. At higher loads and higher sliding distances, the temperature of the worn samples increases, which leads to a higher wear rate, be-

cause of reasons stated above. The EDX analysis done for all these debris indicates the presence of iron as a major constituent, which is shown in Figs. 9a–d.

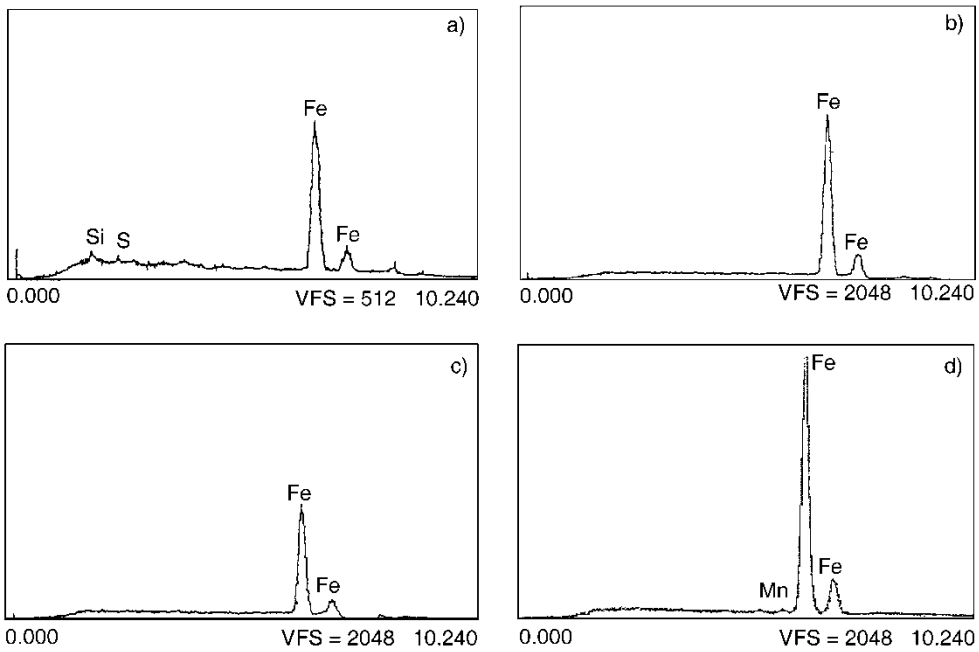

Fig. 9. EDX spectrum of wear debris for: a) AD steel tested at 3.5 kg load, b) ND steel tested at 3.5 kg load, c) IT steel tested at 3.5 kg load, and d) IT steel tested at 5.5 kg load.

Since the morphological features of first linear segment were oxidative in nature and those of second linear segments were primarily metallic in nature, it requires a further confirmation through X-ray diffraction (XRD) analysis. For this purpose, the debris obtained for different steel samples corresponding to first linear segment and second linear segment were separately mixed in a proper way and subject to XRD as presented in Figs. 10a, b for the first and second linear segments, respectively. The analysis indicates that all possible iron oxides (i.e., Fe_2O_3, FeO and Fe_3O_4) are present in debris corresponding to both the segments. Peaks of Fe were also observed in X-ray diffraction pattern.

The consistently higher rate of wear in the first linear segment as compared to that observed in the second linear segment, as shown in Figs. 4a, b, may be explained based on the initial surface roughness of the wearing steel samples. The surfaces of all the engineering components always possess some amount of roughness and have asperities. When a pair of these kinds of fresh surfaces is brought into contact and starts sliding relative to each other, mechanical, chemical, thermal and micro-structural changes begin to occur in and around the contact interface [29]. Due to contact at the asperities, the surfaces evolve to attain better conformity to each other at the end of the run-in stage. The wear in this stage occurs by the removal of high asperities, initial

oxide layers and surface contaminants. Consequently, the material loss and the wear rate are higher in the run-in stage of the wear. In the run-in stage, the oxidation of the surface begins and progresses with frictional heating generated during sliding. The transfer layer of oxide may thus begin to form in the run-in stage and evolves to the steady state, providing an extent of cover determined by the conditions of load, sliding velocity and environmental conditions. The transfer layer protects the underlying metal, and thus the wear rate decreases. The second stage of wear indicates a steady state with respect to (i) the evolution of mating surfaces to better conformity, (ii) the spread of oxide and compacted transfer layer, and (iii) the real area of contact [12]. Sawa and Rigney [5] have also noticed a lower wear rate for DP steels in the steady state as compared to that in the run-in stage.

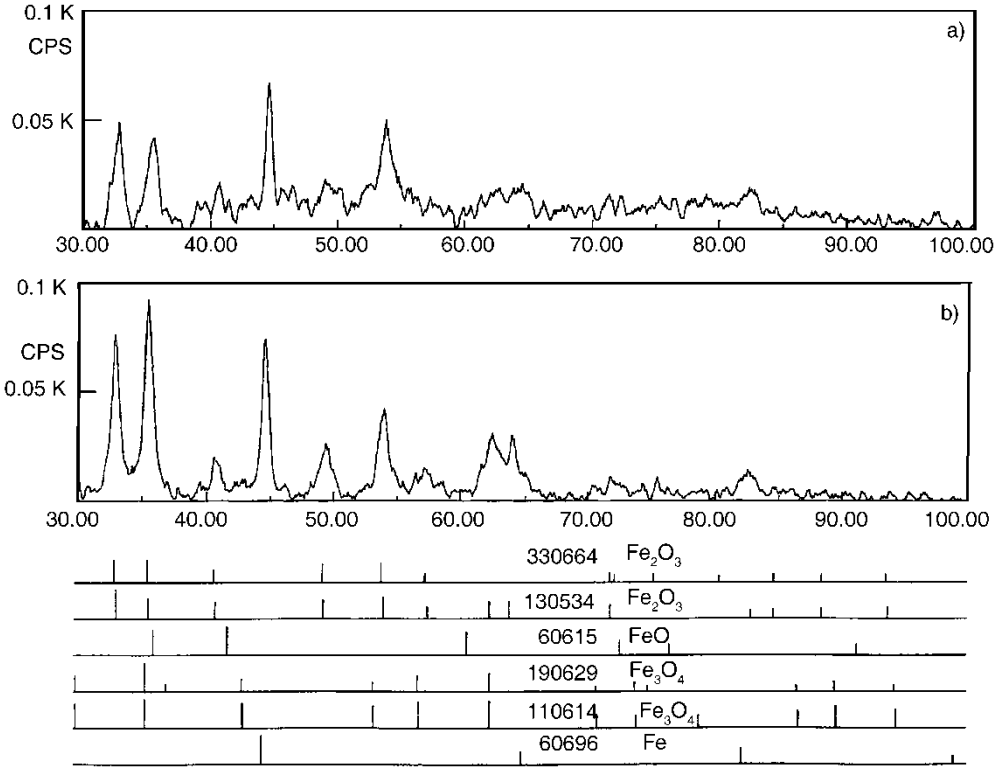

Fig. 10. X-ray diffraction of wear debris of steel samples corresponding to:
a) first linear segment, b) second linear segment

Based on the wear coefficient of both segments, the ferrite–coarse pearlite microstructure has the lowest wear coefficient and it increases in the following order: ferrite–fine pearlite, ferrite–tempered martensite and ferrite–martensite. From these results it appears that relatively coarser cementite plates in coarse pearlite are able to hold out better against sliding wear than the fine cementite plates in fine pearlite. The

masking of fine cementite plates by flow of ferrite could be a contributing factor to increased wear. Fine carbide particles in ferrite-tempere martensite structure are not able to hold out as well as fine cementite plates in fine pearlite. Ferrite-martensite structure appears to be the worst out of all the structures investigated. In spite of its greater hardness, its higher overall adhesion energy may have resulted in its higher wear, as it does not have any carbide in the structure.

The presence of a coarser cementite and cementite plates, as observed in AD and ND steels, rather than particles in IT steel, appears to contribute more wear resistance. The superiority of pearlitic structure over tempered martensitic structure, as observed in this investigation, is well supported by the earlier studies [6–8, 10, 30]. Though, some of the reports mention that higher volume fraction of martensite provides better wear resistance, they do not consider other structural features existing in the system [12, 14]. However, our study further strengthens our previous work carried out on steel with high carbon content [10]. Both the studies, namely the earlier work [10] as well as the present work, are on similar lines and exhibit better understanding with detailed analysis of structural features observed.

4. Conclusions

The present study carried out to determine the influence of microstructure and the morphology of phases in heat treated 0.13 wt. % carbon steel on the dry sliding behaviour against the counter-face of hardened steel has led to the following conclusions:

The volume loss in wear increases with sliding distance and could be described in terms of two linear segments. The wear rate in the first linear segment is higher than that in the second linear segment, which has been attributed to the run-in period in the first segment and progressive development of oxide cover in the second linear segment. The wear rate in both the linear segments increases with load, which is indicative of Archard's wear law.

The mechanism of wear is primarily oxidative, as revealed the analysis of worn surfaces and wear debris. In terms of wear rates of the both segments, ferrite–coarse pearlite structure is superior to ferrite–fine pearlite structure at all the loads. The ferrite–tempered martensite structure results in lower wear rates in both segments compared to ferrite–martensite structure, except at a lower load of 2.5 kg.

Based on the wear coefficients in the first and the second linear segments, the ferrite–coarse pearlite, ferrite–fine pearlite, ferrite–tempered martensite and ferrite–martensite structures in 0.13 wt. % carbon steel show the wear resistance in decreasing order.

References

[1] WELSH N.C., Phil. Trans. Royal Soc. London, A257-31 (1965), 51.
[2] WAYNE S.F., RICE S.L., Wear, 85 (1983), 93.
[3] LIM S.C., ASBY M.F., Acta. Metall., 35 (1987), 1.

[4] LIM S.C., ASBY M.F., BRUNTON J.H., Acta Metall., 35 (1987), 1343.
[5] SAWA M., RIGNEY D.A., Wear, 119 (1987), 369.
[6] PRASAD B.K., PRASAD S.V., Wear, 151 (1991), 1.
[7] WANG Y., PAN L., LEI T.C., Wear, 143 (1991), 57.
[8] GARNHAM J.E., BEYNON J.H., Wear, 157 (1992), 81.
[9] VENKATESHAN S., RIGNEY D, A., Wear, 153 (1992), 163.
[10] GUPTA V.K., PANDEY O.P., Indian J. Eng. Mater. Sci., 7 (2000), 354.
[11] TYAGI R., NATH S.K., RAY S., Metall. Mater. Trans., A32 (2001), 359.
[12] TYAGI R., NATH S.K., RAY S., Metall. Mater. Trans., A33 (2002), 3479.
[13] TYAGI R., NATH S.K., RAY S., Wear, 255 (2003), 327.
[14] TYAGI R., NATH S.K., RAY S., Mater. Sci. Tech., 20 (2004), 645.
[15] MOHAN S., PRAKASH V., PATHAK J.P., Wear, 252 (2002), 16.
[16] DENG S., SUN L., LI Z., Lubr. Eng., 4 (2005), 84.
[17] KAUL R., GANESH P., TIWARI P., NANDEKAR R.V., NATH A.K., J. Mater. Proc. Tech., 167 (2005), 83.
[18] AMAMOTO Y., GOTO H., Tribology Int., 39 (2006), 756.
[19] CESCHINIA L., PALOMBARINIA G., SAMBOGNAA G., FIRRAOB D., SCAVINOB G., UBERTALLIB G., Tribo. Int., 39 (2006), 748.
[20] BAYER R.G., *Mechanical Wear Prediction and Prevention*, Marcel Dekker, New York, 1994.
[21] DEHOFF R.T., RHINES F.N., *Materials Science and Engineering Series*, McGraw-Hill, New York, 1968
[22] CLAYTON P., Wear, 60 (1980), 75.
[23] GLASCOTT J., STOOT F.H., WOOD G.C., Wear, 97 (1984), 155.
[24] SMITH A.F., Wear, 110 (1986), 151.
[25] SMITH A.F., Wear, 123 (1988), 313.
[26] IWABUCHI A., HORI K., KUBOSAWA H., Wear, 128 (1988), 123.
[27] CLARKE J., SARKAR A.D., Wear, 69 (1981), 71.
[28] GLASSER W.A., Wear, 73 (1981), 371.
[29] BLAU P., Wear, 72 (1981), 55.
[30] KALOUSEK J., FEGRADO K.M., LAUFFR E.E., Wear, 105 (1985), 199.

Received 2 September 2007
Revised 7 December 2007